Journal of Hazardous Materials 186 (2011) 240–246

Contents lists available at ScienceDirect

Journal of Hazardous Materials

journal homepage: www.elsevier.com/locate/jhazmat

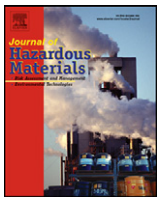

Degradation of natural organic matter in surface water using vacuum-UV irradiation

Gustavo Imoberdorf, Madjid Mohseni*

Department of Chemical and Biological Engineering, University of British Columbia, 2360 East Mall, Vancouver, BC, Canada V6T 1Z3

ARTICLE INFO

Article history:
Received 25 August 2010
Received in revised form 28 October 2010
Accepted 29 October 2010
Available online 9 November 2010

Keywords:
Natural organic matter (NOM)
Water treatment
Vacuum-UV (VUV)
Surface water
Photolysis
Photochemical degradation

ABSTRACT

The use of vacuum-UV (VUV) radiation to degrade natural organic matter (NOM) and the main variables affecting the efficiency of this process were investigated using an annular photoreactor. After 180 min of irradiation with VUV, the total organic carbon (TOC) decreased from 4.95 ppm to 0.3 ppm. Also, decadic absorption coefficients of the water at 185 nm and 254 nm decreased from 3.2 cm^{-1} to 2.85 cm^{-1}, and 0.225 cm^{-1} to 0 cm^{-1}, respectively. The reactor operation was kinetically controlled for Reynolds numbers greater than 600, changes of pH between 5 and 9 had little effect, and increases in alkalinity decreased the process efficacy. Additionally, H_2O_2/VUV and VUV processes were compared to H_2O_2/UV and UV processes, where the formers showed greater effectiveness with complete mineralization of NOM as opposed to partial oxidation with H_2O_2/UV, and no mineralization with UV alone. Modeling and analysis of the photon flux and absorption in the reactor showed that 99% of the 185 nm radiation was absorbed by the water in the reactor. In comparison, only 48% of the 254 nm radiation was absorbed by the water. The overall quantum efficiency of the mineralization for VUV was 0.10 for 50% TOC reduction.

1. Introduction

The presence of natural organic matter (NOM) in water is undesirable because it interferes with drinking water treatments [1,2], contributes to the formation of disinfection by-products (DBPs) such as trihalomethanes and haloacetic acids [3,4], and may induce a subsequent deterioration of water quality due to bacterial regrowth in distribution systems [5]. Advanced oxidation processes (AOPs), such as H_2O_2/UV, O_3/UV, O_3/H_2O_2, and vacuum-UV (VUV) processes, constitute promising technologies that are being studied for the elimination or partial oxidation of NOM in raw water. The VUV process presents the advantage of being chemical free as it does not require any chemical addition. The degradation of organics during the VUV treatment is induced primarily by highly oxidizing hydroxyl radicals ($HO^{\bullet}$) that are generated by the photolysis of water at wavelengths lower than 190 nm [6].

There have been significant research and advances in the past several years on the use of VUV for the degradation of specific water pollutants [6–8]. However, few studies have researched VUV process for the degradation of NOM in aqueous streams. Thomson et al. [9] studied the removal of NOM from water using low pressure Hg lamps and reported that VUV process offered 5 times greater NOM removal efficiency compared to an identical system with UV lamp emitting at 254 nm. The authors also studied the synergetic effect of VUV/UV and H_2O_2 on NOM degradation, and concluded the presence of H_2O_2 increased the rate of NOM degradation. In a separate study, Buchanan et al. [10] observed a fast formation of biodegradable compounds during irradiation with VUV, concluding that a significant reduction of organic matter could be achieved utilizing VUV irradiation followed by biological treatment. The integration of VUV and biological activated carbon was investigated by Buchanan et al. [11], who achieved significant NOM removal along with reductions in trihalomethane and haloacetic acid formation potentials. On the other hand, Dobrović et al. [12] studied the influence of the reactor hydrodynamics on the efficiency of UV, VUV, and H_2O_2/UV processes for the degradation of NOM. The authors observed that the efficiency of the VUV process can be improved by increasing the Reynolds number in the reactor, highlighting the presence of diffusional resistances [12]. All these preliminary studies demonstrate the benefits of applying VUV process to the treatment of surface water containing NOM, and warrant more understanding of the process and its operating parameters.

In this paper, the effectiveness of the VUV radiation for the degradation of NOM is studied. The NOM degradation is analyzed by comparing the results of experiments with UV, H_2O_2/UV, VUV, and H_2O_2/VUV treatments of raw water. Also, the effect of process and water parameters, such as recycling flow rate, pH, and alkalinity are analyzed to determine the relevant variables of the system. Further, a radiation model was used to analyze the usage and distribution of radiative energy and the overall quantum efficiency of the NOM degradation.

* Corresponding author. Tel.: +1 604 822 0047; fax: +1 604 822 6003.
E-mail address: mmohseni@chbe.ubc.ca (M. Mohseni).

0304-3894/$ – see front matter © 2010 Elsevier B.V. All rights reserved.
doi:10.1016/j.jhazmat.2010.10.118

2. Materials and methods

2.1. Raw water samples

Raw water samples were taken in May 2008 from Trepanier Creek, in central British Columbia, Canada. The unfiltered samples were stored at 4 °C prior to use. The pH of the water samples was 7.6, the alkalinity was 40 mg $CaCO_3$ L^{-1}, the decadic absorption coefficients at 254 nm and 185 nm were 0.25 cm^{-1} and 3.20 cm^{-1}, respectively, and the total organic carbon (TOC) concentration was 4.95 mg L^{-1}. This water had a very low content of particulates and only 7% of the TOC could be removed by filtration using 1.4 μm filter.

2.2. Experimental setup and procedure

The photoreactor was made of glass, with an annular configuration. A VUV-Hg lamp (Light Sources Inc. G10T51-2-VH), emitting radiation at 254 and 185 nm, was longitudinally placed at the axial center of the reactor. For some control experiments, a UV-Hg lamp (Light Sources Inc. G10T5-1/2L), which emits practically at 254 nm, was used instead. The external and internal diameters of the annular reactor were 2.5 cm and 1.5 cm, respectively, giving an annulus thickness of 0.5 cm and a total reactor volume of 85 cm^3. The reactor was coupled with a peristaltic pump and a storage tank, allowing for the recirculation of water through the reactor. The storage tank had a porous diffuser for sparging air in the solution.

For each experimental run, 1000 cm^3 of raw water was treated in the photoreactor. For experiments requiring pH modifications, H_2SO_4 or NaOH was added to the water to modify the pH. $NaHCO_3$ was used to increase alkalinity in some tests conducted to study the effect of alkalinity. Finally, except for those experiments where the effect of flow rate was studied, the experiments were conducted with a recycling flow rate of 1000 cm^3 min^{-1}. Some experiments involving VUV were replicated 3 times to assess the reproducibility of the experiments. The standard deviations for the data were less than 5%.

2.3. Analytical methods

The concentration of TOC was measured with a TOC-VCPH Shimadzu analyzer. The concentration of H_2O_2 was measured using the triiodide method [13]. Decadic absorption coefficient at 254 nm (α_{254}) was determined using a UV–Vis spectrophotometer (Shimadzu 1240), whereas decadic absorption coefficient at 185 nm (α_{185}) was measured using a VUV–UV–Vis spectrophotometer (Cary 4000 Varian). For the absorbance measurements at 185 nm, the water samples were degassed (to eliminate O_2 and CO_2). Similarly, degassed Milli-Q water was used as a blank. The decadic absorption coefficient of pure water at 254 nm and 185 nm are 0.0 cm^{-1} and 1.8 cm^{-1} [14], respectively. The total decadic absorption coefficient of raw water at 185 nm was computed considering the absorbance taken using water blanks and the decadic absorption coefficient of water at 185 nm (1.8 cm^{-1}). pH was measured using a pH meter (Thermo Orion PerpHecT LogR 1330 meter, 9206BN electrode) and the concentration of dissolved oxygen in water was monitored with a dissolved oxygen meter (YSI 52 meter, YSI 5909 probe).

The 254 nm radiation flux of the VUV-Hg lamp was measured using a research radiometer (IL 1700, SED240 sensor, and NS254 filter), which was calibrated with the potassium iodide/potassium iodate actinometric technique [15]. The net radiation flux of 254 nm radiation emitted by the VUV-Hg lamp was 37.59 mW cm^{-2}. Finally, the 185 nm radiation flux emitted by the VUV-Hg lamp was determined using the cis–trans cyclooctene photoisomerisation actinometric technique [16]. The measured radiation flux at 185 nm was 3.21 mW cm^{-2}.

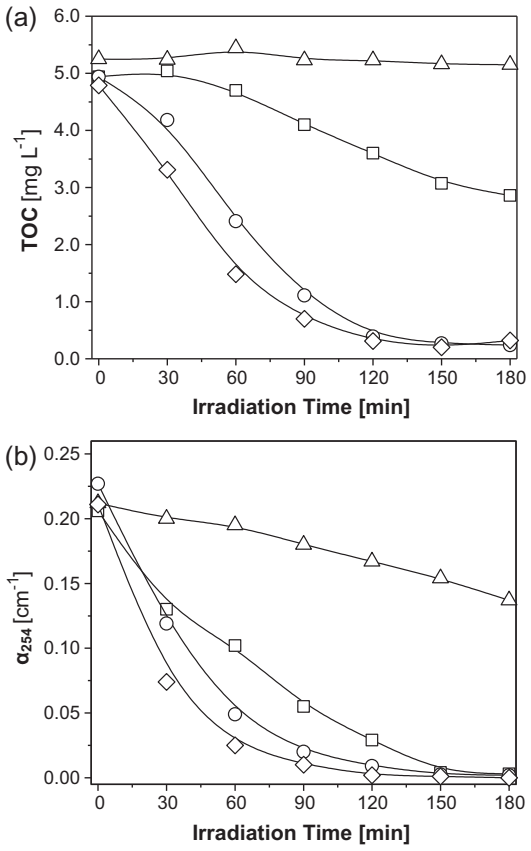

Fig. 1. TOC (a) and α_{254} (b) during the irradiation process of raw water using UV (△), 15 ppm H_2O_2 and UV (□), VUV (○), and 15 ppm H_2O_2 and VUV (◊).

High performance size exclusion chromatography (HPSEC) was used to determine changes in the apparent molecular weight distribution of NOM. A Waters 1535 Binary HPLC Pump fitted with a Waters Protein-PakTM 125 Å column and a Waters 2487 dual λ absorbance detector was used for the analysis. The wavelength of the detector was set at 260 nm. An aqueous solution of 0.02 M phosphate buffer (pH 6.8), adjusted with sodium chloride to 0.1 M ionic strength was used as a carrier solvent (flow rate = 0.7 mL min^{-1}).

3. Results and discussions

3.1. NOM degradation with UV, UV/H_2O_2, VUV, VUV/H_2O_2

Samples of raw water and raw water supplemented with 15 mg L^{-1} of H_2O_2 were irradiated using a UV-Hg or a VUV-Hg lamp (i.e., UV, UV/H_2O_2, VUV, and VUV/H_2O_2 processes). The UV/H_2O_2 process was included as control because this is an established process with significant similarities to the VUV process since both the VUV and the UV/H_2O_2 treatments rely on the oxidizing action of hydroxyl radicals. Batches of 1000 cm^3 of raw water were irradiated for 180 min under different conditions and samples were collected and analyzed at set intervals. The extent of degradation of NOM was analyzed by monitoring the reduction of TOC and α_{254} (Fig. 1a and b).

3.1.1. NOM + UV

As shown in Fig. 1a, no TOC reduction (i.e., mineralization of NOM) was achieved when raw water was irradiated with UV_{254} (without any H_2O_2 addition). Under these conditions, $HO^{\bullet}$ was not

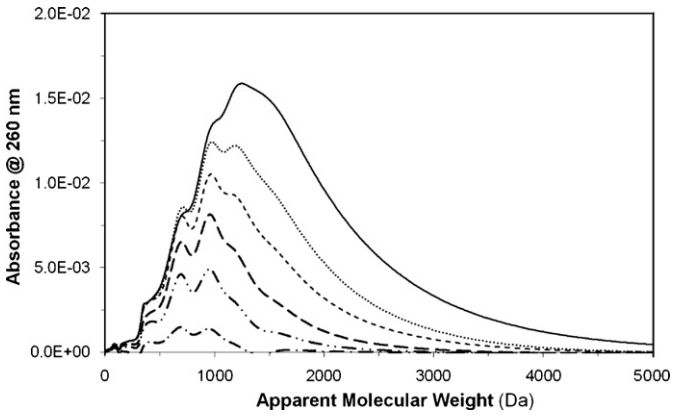

Fig. 2. HPSEC chromatograms of raw water treated by VUV: $t = 0$ (—), $t = 10$ min (·····), $t = 20$ min (- - -), $t = 30$ min (– –), $t = 40$ (– · · –), and $t = 60$ min (– · –).

expected to form because 254 nm radiation could not photolyze water and there was no H_2O_2 in the system. However, structural changes in NOM were observed, as shown by the reduction of α_{254} (Fig. 1b). After 180 min of irradiation, α_{254} decreased by 35% due to the breakdown of the chemical compounds, such as aromatic rings and double bond structures, responsible for absorbing radiation at 254 nm [17]. This observation was also supported by the HPSEC results, indicating changes in the apparent molecular weight distribution of organics (data not shown).

3.1.2. NOM + H_2O_2 + UV

Samples of raw water with 15 mg L^{-1} of H_2O_2 were irradiated with 254 nm UV radiation. As noted in Fig. 1a and b, both TOC and α_{254} decreased as the irradiation time increased. These were the consequence of the degradation of NOM due to the reaction with $HO^\bullet$ generated by the photolysis of H_2O_2 with 254 nm radiation:

$$H_2O_2 + h\nu_{254nm} \rightarrow 2HO^\bullet \quad (1)$$

The mineralization of NOM, which is attributed mostly to the reaction between $HO^\bullet$ and NOM, can be schematically represented as:

$$NOM + HO^\bullet \rightarrow CO_2 + H_2O + \text{Mineral acids} \quad (2)$$

Partial degradation, in which no mineralization occurs, predominated during the initial 30 min of the UV/H_2O_2 process, as represented by nearly constant TOC, yet a significant decrease in α_{254}. Nonetheless, mineralization was observed with further irradiation.

3.1.3. NOM + VUV

The efficiency of NOM degradation with VUV was significantly higher than that obtained with either UV or H_2O_2/UV process (Fig. 1a and b). The TOC started to decrease from the beginning, even though the rate of reduction was slow during the initial 30 min. After the initial period of slow mineralization, the TOC decreased significantly from about 4.2 mg L^{-1} to 0.3 mg L^{-1} after 120 min of irradiation. Unlike TOC, α_{254} started to decrease immediately, indicating major changes in the structure and composition of NOM. Comparing Figs. 1a and 2b underscores the existence of series of reactions that start with the partial breakdown of NOM, due to photolysis or reaction with $HO^\bullet$, followed by complete mineralization. In other words, these results suggest that the complex and large molecules of NOM are first degraded and broken down to smaller molecules with lower molar absorption coefficients at 254 nm. The smaller and less complex molecules are subsequently mineralized by the action of $HO^\bullet$ and other oxidizing species. This interpretation is in full agreement with the results obtained by Thomson et al. [9] who observed no changes in TOC, but a significant reduction of α_{254} in the initial stages of VUV irradiation.

The values of α_{185} were measured during the treatment of raw water with VUV (not shown). The initial α_{185} of raw water was 3.2 cm^{-1}. This high decadic absorption coefficient is a consequence of not only the decadic absorption coefficient of water (1.8 cm^{-1}), but also the absorbance of organic and inorganic species (e.g., carbonates and bicarbonates, phosphates, and other ions), which have high molar absorption coefficients at 185 nm. A slow but steady reduction of α_{185} was observed during the treatment. After 3 h of VUV irradiation, α_{185} was 2.85 cm^{-1}, which represents a relatively small reduction of about 10% when compared with the total TOC reduction of about 94% or with the α_{254} reduction of nearly 100%. This difference will be analyzed in details in the following section using the radiation model.

Changes in the apparent molecular weight distribution of NOM where analyzed with HPSEC. Fig. 2 shows the HPSEC chromatograms obtained for the untreated water and water treated with VUV for up to 1 h. HPSEC results show high molecular weight compounds were gradually degraded right from the beginning of the process, but there were little changes in low molecular weight compounds. After 30, 40, and 60 min of irradiation, a progressive reduction in the concentration of both high and low molecular weight compounds took place.

The most important reactions taking place during the VUV process were described and discussed by Gonzalez et al. [6]. Two of such reactions for the VUV/water system are the photochemical homolysis of water:

$$H_2O + h\nu_{185nm} \rightarrow HO^\bullet + H^\bullet \quad (3)$$

and the photochemical ionization of water:

$$H_2O + h\nu_{185nm} \rightarrow HO^\bullet + H^+ + e^- \quad (4)$$

The quantum yields for the photochemical homolysis and ionization of water at 185 nm are 0.33 and 0.045, respectively [6]. The strong oxidizing $HO^\bullet$ may react not only with the organic and inorganic compounds present in raw water, but also with other radicals. Hydroxyl radicals can also react among themselves to produce H_2O_2, which itself reacts with $HO^\bullet$ to produce $HO_2^\bullet/O_2^{\bullet-}$. Besides, $HO_2^\bullet/O_2^{\bullet-}$ are produced via the reaction between $H\cdot$ and O_2, and the reaction between e^- and O_2. Also, $HO_2^\bullet/O_2^{\bullet-}$ may react with one another to produce H_2O_2. Details of all the reactions between the radicals are discussed by Gonzalez et al. [6].

Another important reaction occurring in the system is the photolysis and photochemical reaction of NOM by 185 nm radiation:

$$NOM + h\nu_{185nm} \rightarrow \text{products} \quad (5)$$

3.1.4. NOM + H_2O_2 + VUV

A further improvement in the NOM degradation was observed when 15 mg L^{-1} of H_2O_2 was added to the raw water, irradiated with the VUV-Hg lamp. In this case, $HO^\bullet$ is generated not only by the photolysis of water at 185 nm, but also by the photolysis of H_2O_2 induced by 185 and 254 nm radiation. The photolysis of H_2O_2 at 185 and 254 nm is beneficial because of the additional formation of $HO^\bullet$. Therefore, the overall rate for reaction (2) in the VUV/H_2O_2 process is expected to increase compared to that in the VUV process.

3.2. Effect of operating variables and water quality characteristics

3.2.1. Effect of Reynolds number

For this set of experiments, the reactor was operated with different recycling flow rates to determine the potential existence of diffusive resistances. The range of recycling flow rate was between 150 and 3000 cm^3 min^{-1} (Re = 89 to 1780); hence, the hydraulic residence time per pass ranged between 32 s and 1.6 s. Although the

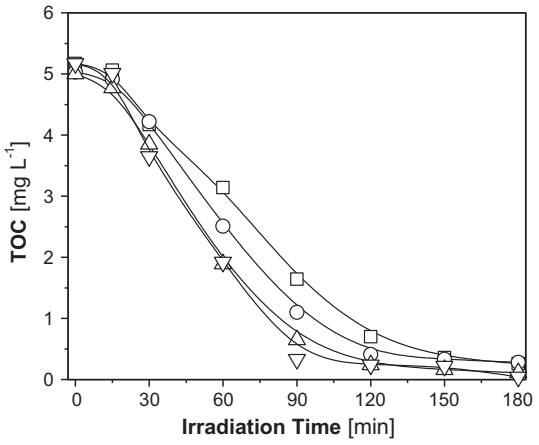

Fig. 3. TOC evolution during the VUV irradiation process of raw water using recycling flow rate of 150 mL min^{-1} (or Re = 89) (□), 300 L min^{-1} (or Re = 178) (○), 1 L min^{-1} (or Re = 600) (△), 3 L min^{-1} (or Re = 1781) (▽).

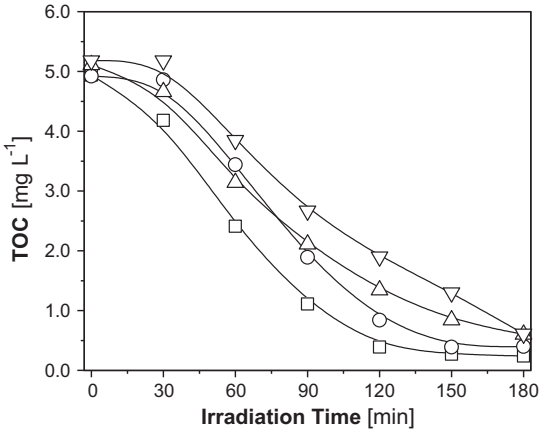

Fig. 5. TOC evolution during the VUV irradiation process of raw water with different alkalinities: 40 mg $CaCO_3$ L^{-1} (□), 100 mg $CaCO_3$ L^{-1} (○), 200 mg $CaCO_3$ L^{-1} (△), 300 mg $CaCO_3$ L^{-1} (▽).

reactions taking place in the VUV process are homogeneous, the high absorption coefficient of water at 185 nm generates a steep gradient of the radiation flux and therefore, the rate of photon absorption and the subsequent photochemical reaction rates are expected to be much higher close to the lamp, leading to potential mass transfer limitations. Fig. 3 shows that similar rates of TOC reduction were observed for the Reynolds number of 600 or higher. However, experiments conducted with two lower Reynolds numbers (i.e., smaller than 600) showed slower mineralization rates. Under the operating conditions used, the flow regime was laminar (Re < 2300). Even though no significant changes in the flow characteristics were expected in the range of Reynolds numbers applied, experimental results indicate that diffusion resistances were negligible for Reynolds numbers greater than 600. These flow rates generated an appropriate mixing in the reactor most likely because of the convective flow of the oxygen and NOM. Hence, all the subsequent experiments were conducted with a flow of 1000 cm min^{-1}, corresponding to Re = 600, without major concern related to diffusion resistances.

3.2.2. Effect of pH

A number of experiments were conducted with raw waters at pH values of 5, 7, and 9. pH adjustments were made by adding appropriate amounts of H_2SO_4 and NaOH, for acidic and alkaline pH, respectively. As seen in Fig. 4, the results suggest that moderate

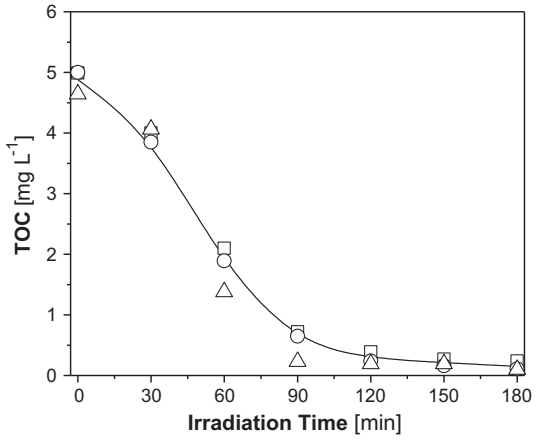

Fig. 4. TOC evolution during the VUV irradiation process of raw water at pH 5 (◊), pH 7 (△), pH 9 (□).

variations on the pH have little impact on NOM degradation efficiency. Similar observations were reported by Stefan et al. [18] who studied the degradation of acetone using H_2O_2/UV. The authors concluded that no acid-catalyzed reactions occur in the system.

3.2.3. Effect of alkalinity

The impact of alkalinity on the VUV process was investigated by adding different amounts of $NaHCO_3$ to the raw water. As expected, the higher the alkalinity of the water, the lower the rate of TOC reduction (Fig. 5). This was clearly because carbonates and bicarbonates: (i) act as scavengers of HO$^\bullet$ and hence, reduce the concentration of HO$^\bullet$ available to degrade NOM, and (ii) absorb 185 nm radiation, increasing the attenuation of radiation in the reactor, thereby reducing the photons available for the photolysis of water.

Carbonates and bicarbonates may react with HO$^\bullet$ according to:

$$HO^\bullet + CO_3^{2-} \rightarrow CO_3^{-\bullet} + HO^- \quad (6)$$

$$HO^\bullet + HCO_3^- \rightarrow CO_3^{-\bullet} + H_2O \quad (7)$$

The kinetic constants of reactions (6) and (7) are $k_6 = 3.9 \times 10^8$ M^{-1} s^{-1} and $k_7 = 8.5 \times 10^6$ M^{-1} s^{-1} respectively [19]. The kinetic constant of the reaction between NOM and HO$^\bullet$, based on moles of organic carbon, is in the range of 1.6×10^8 to 3.7×10^8 M^{-1} s^{-1} [20,21]. The initial molar concentrations of organic carbon and that of bicarbonates/carbonates in the raw water employed were 0.41 and 0.40 mmol L^{-1}, respectively. Thus, carbonates and bicarbonates were expected to compete with NOM for reaction with HO$^\bullet$.

As for the attenuation effect, both bicarbonates and carbonates absorb 185 nm radiation, even at very low concentrations. The molar absorption coefficient of carbonates and bicarbonates at 185 nm are 1.75×10^3 L mol^{-1} cm^{-1} and 1.10×10^3 L mol^{-1} cm^{-1}, respectively [14]. For example, when the concentration of carbonates and bicarbonates is 40 ppm, their contribution to the total decadic absorption coefficient will be $\alpha_{CO_3,185} = 0.7$ cm^{-1} and $\alpha_{HCO_3,185} = 0.44$ cm^{-1}, respectively, which are comparable to that of water at 185 nm (i.e., 1.8 cm^{-1}). For this reason, for alkalinity being in the range of 40 mg L^{-1} or higher (e.g., the raw water used in this study), carbonates and bicarbonates compete with water for 185 nm photons, and therefore, an additional adverse effect on the effectiveness of the VUV process will be expected.

3.3. Radiation field

When modeling the radiative energy propagation in a system in which the radiation is not comprised of parallel beams, the Beer-Lambert law cannot be used. This is particularly the case for annular photoreactors where the lamp is placed at the center. The radiation field of such systems may be preferentially modeled by solving the radiative transfer equation [22].

Prior to describing the radiation model, the variables that were used to analyze the radiation field are defined. The local net spectral radiation flux and the spectral incident radiation are defined as:

$$q_\lambda(\underline{x}) = \int_\Omega I_\lambda(\underline{x}, \underline{\Omega})\underline{\Omega} \cdot \underline{n}_s \cdot d\Omega \tag{8}$$

$$G_\lambda(\underline{x}) = \int_\Omega I_\lambda(\underline{x}, \underline{\Omega}) d\Omega \tag{9}$$

where $I_\lambda(\underline{x}, \underline{\Omega})$ is the specific spectral radiation intensity that reaches a given point located at position $\underline{x}$, $\underline{n}_s$, is the normal vector with respect to the cylindrical surface coaxial with the reactor and lamp axes, and Ω is the solid angle. The local volumetric rate of photon absorption [23], $e^{a,\nu}_\lambda$, is defined as follows:

$$e^{a,\nu}_\lambda(\underline{x}) = \alpha_\lambda G_\lambda(\underline{x}) \ln(10) \tag{10}$$

where α_λ is the decadic spectral absorption coefficient of the propagating medium.

The photon absorption distribution was evaluated using the Monte Carlo (MC) method [24], which involves tracking the trajectory of a large number of photons and computing the location where they are absorbed. The model was solved independently for the two wavelengths emitted by the VUV-Hg lamp (i.e., 185 nm and 254 nm). For each simulation, 10^7 photons were considered. The net emission power of the lamp was evaluated by actinometry, giving the values:

$$P_{L,185} = 0.48\,\text{W} \tag{11}$$

$$P_{L,254} = 5.66\,\text{W} \tag{12}$$

Once the absorption point of all the photons were known, the $e^{a,\nu}$ was evaluated as follows:

$$e^{a,\nu}_\lambda(r) = P_{L,\lambda} \frac{n_{ph,abs}(r)}{n_{ph,tot}} \frac{1}{V_{elem}(r)} \tag{13}$$

where $n_{ph,abs}$ is the number of photons absorbed in a given element of the reactor located at a distance equal to r, $V_{elem}(r)$ is the volume of such element, and $n_{ph,tot}$ is the total number of photons considered in the MC model.

The local net spectral radiation flux at different positions was evaluated as:

$$q_\lambda(r) = P_{L,\lambda} \frac{n_{ph,trans}(r)}{n_{ph,tot}} \frac{1}{L_R \pi 2r} \tag{14}$$

where $n_{ph,trans}$ is the number of photons transmitted through a cylindrical surface with radius equal to r.

The local radiation flux in the photoreactor was calculated considering the optical properties of the raw water after different irradiation times. Radial profiles of the radiation flux for 254 nm and 185 nm are presented in Fig. 6a and b, respectively. In all the cases, the maximum values of the net radiation flux are located in the layer of water in contact with the internal wall of the reactor, next to the lamp. As the distance of a given point from the lamp increases, lower values are obtained for the radiation flux. At the beginning of the process, the decadic absorption coefficient of raw water at 254 nm was 0.225 cm^{-1}; however, as shown in Fig. 1b, α_{254} decreased with time, leading to the modification of the radiation field. Fig. 6a shows the net radiation flux obtained considering

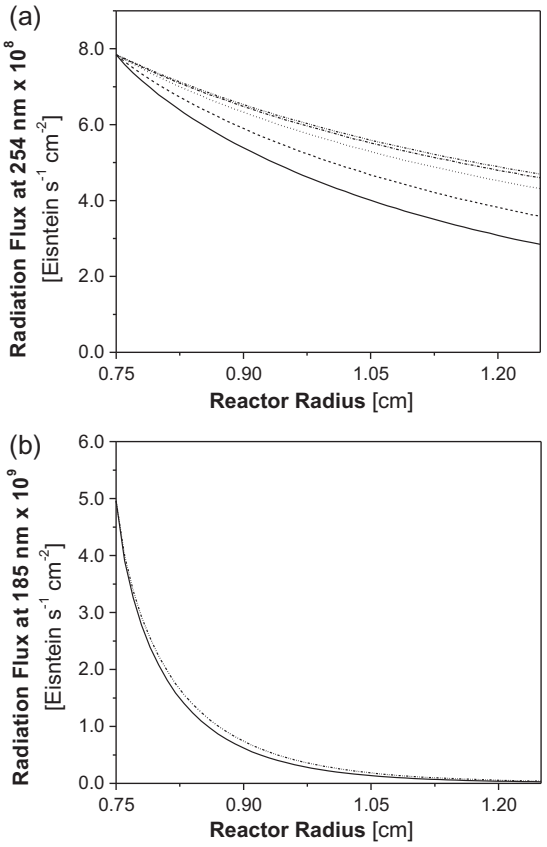

Fig. 6. Radial radiation flux profiles for 254 nm (a) at $t = 0$ (—), $t = 30$ min (- - -), $t = 60$ min (·····), $t = 120$ min (– · –), and $t = 180$ min (– · · –). Radial radiation flux profiles for 185 nm (b) at $t = 0$ (—) and $t = 180$ min (– · · –).

the reductions in the α_{254} of water after 30, 60, 120, and 180 min. The gradients of radiation flux decreased with increasing the irradiation time because of the reductions in α_{254}. Indeed, the α_{254} was practically negligible after 180 min of irradiation (Fig. 1b), a fact that was supported by modeling. According to the modeling results, 48% of the 254 nm radiation was absorbed by raw water at the beginning of the process, whereas practically no 254 nm radiation was absorbed after 180 min of irradiation. However, despite the negligible α_{254} Fig. 6a shows some non-uniformities and gradients of the radiation flux across the reactor. These gradients of the radiation flux after extended irradiations are exclusively due to the divergence of radiation in the annular geometry.

The decadic absorption coefficient of raw water at 185 nm was very high (about 3.2 cm^{-1}), which reduced the penetration of 185 nm radiation. Accordingly, steep gradients on the net radiation flux were obtained (Fig. 6b). The decadic absorption coefficient of raw water prior to the treatment was 3.2 cm^{-1}, and it decreased to 2.85 cm^{-1} after 180 min of irradiation, corresponding to a net reduction of 0.35 cm^{-1} (i.e., 10% reduction). For this reason, no significant changes were obtained for the radiation flux profiles at different irradiation times (Fig. 6b).

As previously noted, the α_{185} of initial raw water was 3.2 cm^{-1}, which was 1.4 cm^{-1} higher than that of pure water (1.8 cm^{-1}). The difference corresponds to the absorbance of organic compounds (NOM) and inorganic species present in raw water (carbonates, bicarbonates, phosphates, etc.). With the TOC of the treated water being very low (0.3 mg L^{-1}), one could associate the reduced decadic absorption coefficient of 0.35 cm^{-1} (= 3.2 cm^{-1} – 2.85 cm^{-1}) to the absorption of NOM. Also, the remaining 1.05 cm^{-1} (= 3.2 cm^{-1} – 1.8 cm^{-1} – 0.35 cm^{-1}) could be associated with the absorbance of inorganic compounds, such as

carbonates or bicarbonates. Hence, it may be concluded that at the beginning of the process, about 56% of the 185 nm radiation was absorbed by water molecules, about 33% by inorganic compounds, and about 11% by NOM. After 180 min of irradiation, about 63% of the 185 nm photons were absorbed by water molecules, with the rest being absorbed by inorganic compounds.

In general terms, previous results show that the efficiency of the VUV process for the degradation of NOM depends on not only the operating conditions of the photoreactor, but also the quality of the water being treated. The level of carbonates and other inorganic species affects the propagation of VUV photons. Additionally, carbonates act as scavengers for HO•, reducing the availability of HO• to react with NOM.

3.4. Quantum efficiency

Given the complexity of the system under study, the quantum yield cannot be used to analyze the photon usage for the degradation of NOM. Instead, quantum efficiency was defined as the ratio between the rate of mineralization and the rate of photon absorption at a given wavelength:

$$\Theta_\lambda = \frac{\text{rate of mineralization}}{\text{rate of photon absorption}} \quad (15)$$

The concept of quantum efficiency based on the TOC has been previously used in scientific publications [25]. To consider the particular characteristics of the system under study, some considerations were taken into account:

(1) In this research, a VUV-Hg lamp emitting at 185 nm and 254 nm was used to mineralize NOM via HO• generated by water photolysis. However, the effect of 254 nm radiation was negligible when compared to that of 185 nm (as shown in Fig. 1a, photolysis with 254 nm did not mineralize NOM under the operating conditions studied). Therefore, only the 185 nm photons were considered for the calculation of quantum efficiency.

(2) Given the interests in the mineralization of NOM and that the chemical composition of NOM was unknown, the overall quantum efficiency was calculated considering the number of moles of CO_2 produced during the irradiation process. This was equivalent to the rate of TOC reduction times the volume of raw water treated and then divided by the molecular weight of the carbon.

$$\text{rate of mineralization} = -\frac{d[\text{TOC}]}{dt}\ \frac{V_W}{MW_C} \quad (16)$$

where $d[\text{TOC}]/dt$ is the rate of TOC reduction, V_W is the total volume of water treated (i.e., 1000 cm^3), and MW_C is the molecular weight of carbon.

(3) From our experimental results, the initial mineralization rate was very low, but this value is not representative of the entire process because after 15–30 min, the mineralization reaction rate increased significantly (Fig. 1a). Hence, the numerator and denominator of equation (15) were integrated to calculate the overall quantum efficiency corresponding to the 50% of mineralization [26]:

$$\left\langle \Theta_{185\text{nm}} \right\rangle^{\text{TOC}}_{\text{Overall},t_{1/2}} = \frac{\Delta[\text{TOC}]V_W}{\int_{V_R} e^{a,\nu}_{185\text{nm}}(r)dV_R t_{1/2} MW_C} \quad (17)$$

where ΔTOC is the variation of TOC (in this case, ΔTOC = 50% of the initial TOC), and $t_{1/2}$ is the time required for 50% mineralization. Under the conditions evaluated, the $t_{1/2}$ was 56 min. Finally, the overall quantum efficiency was obtained to be:

$$\left\langle \Theta_{185\text{nm}} \right\rangle^{\text{TOC}}_{\text{Overall},t_{1/2}} = 0.10 \quad (18)$$

The inverse of the quantum efficiency represents the overall number of photons required to mineralize an atom of organic carbon or, that is to say, to generate a molecule of CO_2. Therefore, about 10 photons are required to produce one molecule of CO_2 from NOM. Under this approach, the overall quantum efficiency includes the effect of 185 nm photons that are absorbed by inorganic compounds, the recombination and scavenging of HO•, and all the effects taking place in the photoreactor.

4. Conclusions

The aim of the present paper was to study the effectiveness of VUV process to degrade NOM present in raw waters. The conclusions can be summarized as follows:

- VUV is effective at degrading NOM. After 180 min of irradiation, the TOC of raw water decreased from 4.95 mg L^{-1} to 0.3 mg L^{-1}, decadic absorption coefficient at 254 nm reduced from 0.225 cm^{-1} to almost zero, whereas the decadic absorption coefficient at 185 nm reduced from 3.2 cm^{-1} to 2.85 cm^{-1}.
- The effectiveness of VUV process was compared to those of UV, UV/H_2O_2 and VUV/H_2O_2. The VUV process was much more effective than the UV and UV/H_2O_2 processes, and its effectiveness was enhanced with the addition of H_2O_2.
- Analysis of the radiation propagation inside the VUV reactor showed that 99% of the 185 nm radiation was absorbed by raw water in the reactor volume, whereas only 48% of the 254 nm radiation was absorbed.
- Using the kinetic data and the radiation model, the overall quantum efficiency corresponding to the 50% mineralization of NOM in raw water was calculated to be 0.10.
- The efficiency of the VUV process for the degradation of NOM depends on initial water quality. It was observed that inorganic compounds present in the water samples (e.g., carbonates and bicarbonates) play an important role in the radiation propagation, because they can block the radiation propagation at 185 nm.

Further studies are needed to better understand the complex interaction between VUV, water and NOM.

Acknowledgments

The authors are grateful to BI Pure Water (Canada) Inc., and the Natural Sciences and Engineering Research Council of Canada (NSERC) for their financial support. Thanks also to Neda Abdollahzadeh for her valuable participation in the experimental work.

References

[1] D. Bursill, J. van Leeuwen, M. Drikas, Problems related to particulate and dissolved components in water: the importance of organic matter, Water Supply 2 (2002) 155–162.
[2] P.T. Srinivasan, T. Viraraghavan, Influence of natural organic matter (NOM) on the speciation of aluminum during water treatment, Water Air Soil Pollut. 152 (2004) 35–54.
[3] S.W. Krasner, M.J. McGuire, J.G. Jacangelo, N.L. Patania, K.M. Reagan, E.M. Aieta, The occurrence of disinfection by-products in US drinking water, Am. Water Works Assoc. 81 (1989) 41–53.
[4] A.D. Nikolaou, T.D. Lekkas, The role of natural organic matter during formation of chlorination by-products: a review, Acta Hydroch. Hydrob. 29 (2001) 63–77.
[5] W. Zhang, F.A. DiGiano, Comparison of bacterial regrowth in distribution systems using free chlorine and chloramine: a statistical study of causative factors, Water Res. 36 (2002) 1469–1482.
[6] M.G. Gonzalez, E. Oliveros, M. Woerner, A.M. Braun, Vacuum-ultraviolet photolysis of aqueous reaction systems, J. Photochem. Photobiol. C 5 (2004) 225–246.
[7] G. Baum, T. Oppenlaender, Vacuum-UV-oxidation of chloroorganic compounds in an excimer flow through photoreactor, Chemosphere 30 (2005) 1781–1790.
[8] V.V. Tarasov, G.S. Barancova, N.K. Zaitsev, Z. Dongxiang, Photochemical kinetics of organic dye oxidation in water, Trans. IChemE. 81 (2003) 243–249.

[9] J. Thomson, F. Roddick, M. Drikas, Natural organic matter removal by enhanced photooxidation using low pressure mercury vapour lamps, Water Sci. Technol. Water Supply 2 (2002) 435–443.
[10] W. Buchanan, F. Roddick, N. Porter, Removal of VUV pre-treated natural organic matter by biologically activated carbon columns, Water Res. 42 (2008) 3335–3342.
[11] W. Buchanan, F. Roddick, N. Porter, M. Drikas, Enhanced biodegradability of UV and VUV pre-treated natural organic matter, Water Sci. Technol. Water Supply 4 (2004) 103–111.
[12] S. Dobrović, H. Juretić, N. Ružinski, Photodegradation of natural organic matter in water with UV irradiation at 185 and 254 nm: importance of hydrodynamic conditions on the decomposition rate, Separ. Sci. Technol. 42 (2007) 1421–1432.
[13] N.V. Klassen, D. Marchington, H.C.E. McGowan, H_2O_2 determination by the I_3^- method and by $KMnO_4$ titration, Anal. Chem. 66 (1994) 2921–2925.
[14] J.L. Weeks, G.M.A.C. Meaburn, S. Gordon, Absorption coefficients of liquid water and aqueous solution in the far ultraviolet, Radiat. Res. 19 (1963) 559–567.
[15] R.O. Rahn, Potassium iodide as a chemical actinometer for 254 nm radiation: use of iodate as an electron scavenger, Photochem. Photobiol. A. 66 (1997) 450–465.
[16] H.-P. Schuchmann, C. von Sonntag, R. Srinivasan, Quantum yields in the photolysis of cis-cyclooctene at 185 nm, J. Photochem. 15 (1981) 159–162.
[17] S.R. Sarathy, M. Mohseni, The impact of UV/H_2O_2 advanced oxidation on molecular size distribution of chromophoric natural organic matter, Environ. Sci. Technol. 41 (2007) 8315–8320.
[18] M. Stefan, A. Hoy, J. Bolton, Kinetics and mechanism of the degradation and mineralization of acetone in dilute aqueous solution sensitized by the UV photolysis of hydrogen peroxide, Environ. Sci. Technol. 30 (1996) 2382–2390.
[19] G.V. Buxton, C.L. Greenstock, W.P. Helman, A.B. Ross, Critical review of rate constants for reactions of hydrated electrons, hydrogen atoms and hydroxyl radicals (OH/O^-) in aqueous solution, J, Phys. Chem. Ref. Data 17 (1988) 513–886.
[20] P. Westerhoff, G. Aiken, G. Amy, J. Debroux, Relationships between the structure of natural organic matter and its reactivity towards molecular ozone and hydroxyl radicals, Water Res. 33 (1999) 2265–2276.
[21] J.V. Goldstone, M.J. Pullin, S. Bertilsson, B.M. Voelker, Reactions of hydroxyl radical with humic substances: bleaching, mineralization, and production of bioavailable carbon substrates, Environ. Sci. Technol. 36 (2002) 362–372.
[22] M.M. Ozisik, Radiative Transfer and Interactions with Conduction and Convection, Wiley, New York, 1973.
[23] A.E. Cassano, C.A. Martín, R.J. Brandi, O.M. Alfano, Photoreactor analysis and design: fundamentals and applications, Ind. Eng. Chem. Res. 34 (1995) 2155–2201.
[24] G.E. Imoberdorf, F. Taghipour, M. Keshmiri, M. Mohseni, Predictive radiation field modeling for fluidized bed photocatalytic reactors, Chem. Eng. Sci. 63 (2008) 4228–4238.
[25] G. Waldnera, J. Krýsab, Photocurrents and degradation rates on particulate TiO_2 layers: effect of layer thickness, concentration of oxidizable substance and illumination direction, Electrochim. Acta 50 (2005) 4498–4504.
[26] C.S. Zalazar, M.L. Satuf, O.M. Alfano, A.E. Cassano, Comparison of H_2O_2/UV and heterogeneous photocatalytic processes for the degradation of dichloroacetic acid in water, Environ. Sci. Technol. 42 (2008) 6198–6204.